Environmental Science
Water Research & Technology

ROYAL SOCIETY OF CHEMISTRY

PAPER

Published on 29 January 2020
Licence and permissions

Check for updates

Cite this: *Environ. Sci.: Water Res. Technol.*, 2020, **6**, 1044

Rapid degradation of PFAS in aqueous solutions by reverse vortex flow gliding arc plasma†

Asa J. Lewis,[a] Thomas Joyce,[a] Maher Hadaya,[a] Farshad Ebrahimi,[f] Ivan Dragiev,[a] Nickolas Giardetti,[a] Junchun Yang,[e] Gregory Fridman,[cde] Alexander Rabinovich,[bc] Alexander A. Fridman,[bc] Erica R. McKenzie[f] and Christopher M. Sales *[a]

Poly- and perfluoroalkyl substances (PFAS) are a group of fluorinated organic anthropogenic chemicals that are resistant to degradation. In this paper, non-equilibrium, reverse vortex gliding arc plasma (GAP) discharges in air, nitrogen (N_2), and pure oxygen (O_2) gases were investigated for the removal of perfluoroalkyl carboxylates (PFCA), perfluoroalkyl sulfonates (PFSA), and fluorotelomer sulfonates (FtS) from liquid solutions in a 1-liter treatment system. At initial concentrations ranging from 0.05 g L^{-1} to 1 g L^{-1} significant removal was observed for all PFAS compounds by GAP discharges in air, but the degree of degradation and defluorination was highly dependent on perfluorinated alkyl chain lengths, with all those containing 8 or more perfluorinated carbons achieving greater than 90% removal and often greater than 25% defluorination in one hour of treatment time. Following treatment, a fluorine mass balance was attempted for PFOS (58.3% recovery) and PFOA (98.2% recovery) where only a miniscule portion (5.6% and 4.2%) respectively of the degraded PFOS and PFOA were converted to quantifiable PFAS, while the rest of the fluorine may leave as gaseous species or non-quantifiable PFAS. The non-equilibrium GAP discharge used in this study was found to use similar amounts of energy to other studies using non-equilibrium plasma (150 kJ L^{-1} to 1000 kJ L^{-1}), which is approximately three to twenty times less than the amount of energy used to evaporate water (~3000 kJ L^{-1}). Assuming pseudo-first-order kinetics, the figure-of-merit electrical energy per order (E_{Eo}) values were calculated to estimate the energy efficiency of the system. The lowest E_{Eo} for PFOS was 23.2 kW h m^{-3} per order and 213.4 kW h m^{-3} per order for PFOA, similar with existing technologies (which range from 10 to 10 000 kW h m^{-3} per order). These results indicate that non-thermal air plasma discharges are promising technologies for treatment of PFAS that should be further researched and developed.

Received 26th November 2019,
Accepted 28th January 2020

DOI: 10.1039/c9ew01050e

rsc.li/es-water

Water impact

Per- and polyfluorinated substances (PFAS) are a class of xenobiotic compounds that have contaminated the environment through human activity and production. PFAS are found in drinking water, groundwater, and are not substantially removed by traditional water treatment technologies. Non-equilibrium plasma technologies generate reactive species that can destroy PFAS compounds in water, providing a potential solution to this issue.

Introduction

Poly- and perfluoroalkyl substances (PFAS) are a class of organofluorine compounds that are persistent in the environment, bioaccumulative, and can be soluble in aqueous matrices.[1,2] PFAS are thermally stable, lipid and water repelling, and have been deemed "forever chemicals[3]". PFAS have been liberally used over the past 60 years in aqueous film forming foam (AFFF), household products such as carpets, paper, and non-stick cookware, and even coated cardboard takeout containers.[4–7] Extensive groundwater and surface water

[a] *Department of Civil, Architectural, and Environmental Engineering, Drexel University, Philadelphia, PA 19104, USA. E-mail: chris.sales@drexel.edu*
[b] *Department of Mechanical Engineering and Mechanics, Drexel University, Philadelphia, PA 19104, USA*
[c] *C&J Nyheim Plasma Institute, Drexel University, Camden, NJ 08103, USA*
[d] *AAPlasma LLC, USA*
[e] *School of Biomedical Engineering, Sciences, and Health Systems, Drexel University, Philadelphia, PA 19104, USA*
[f] *Department of Civil and Environmental Engineering, Temple University, Philadelphia, PA 19122, USA*
† Electronic supplementary information (ESI) available. See DOI: 10.1039/c9ew01050e

This journal is © The Royal Society of Chemistry 2020

contamination of PFAS originates from a variety of sources, including industrial and commercial manufacturing plants that produce or use PFAS,[8–10] contaminated biosolids application,[11–13] contaminated landfill leachate,[14–17,26] wastewater and water treatment plants discharges,[18–21,27] and AFFF training facilities.[6,22,23,28–31] Drinking water supplies for millions of U.S. residents have been contaminated with various PFAS, with both perfluorooctanesulfonic acid (PFOS) and perfluorooctanoic acid (PFOA) often surpassing the US EPA's lifetime health advisory (70 ng L^{-1}).[24] Since this advisory was set for these two compounds, most research done to date focuses on PFOS and PFOA, but a growing number of studies are investigating a wider range of PFAS, including perfluorocarboxylic acids (PFCA), perfluorosulfonic acids (PFSA), fluorotelomer sulfonates (FtS), and a number of unknown precursor PFAS compounds[22,25] that are also present in the contaminated water.

Due to PFAS contamination in groundwater, surface water, agriculture, and drinking water and their associated health risks,[4,24,32–38] there has been a great focus on developing practical and effective water treatment technologies. Treatment technologies developed so far have included adsorptive and destructive methods. Some PFAS can associate strongly to proteins through either electrostatic or non-electrostatic (hydrophobic/hydrophilic) physisorption as well as site specific chemisorption.[39,40] Based off these properties, adsorptive methods have been developed to remove these specific compounds from water but are not effective for all PFAS compounds.[41] Adsorptive methods to date include granular activated carbon (GAC),[42] ion exchange (IX),[43,44] polymers,[45] and protein addition.[46] These methods show promise in effectively removing some of the compounds from contaminated water but can be expensive and do not degrade the PFAS compound, leading to the generation of PFAS contaminated residues and concentrates.

Due to the recalcitrant nature of PFAS and the C–F bond, destructive methods development has come with difficulties. Destructive method of PFAS in contaminated water that have been studied for their treatment ability include sonolysis,[47–50] thermal degradation,[51] photocatalytic ozonation,[52] electrochemical oxidation,[53–56] persulfate,[51,57–59] alkaline hydrothermal treatment,[60] microwave/persulfate,[61] UV,[62,63] ionizing radiation electron beam,[64] γ-irradiation,[65] boron-doped diamond film electrode oxidation,[66] electrical discharge plasma,[67] and biodegradation.[68] Novel reductive processes such as photogenerated hydrated electrons (e^-_{aq})[69–71] are also being developed as a treatment technology. These methods described above have been demonstrated to be effective in degradation and lead to varying degrees of destruction involving reduction in chain length, cleaving of C–F bond, and removal of head group.

A promising treatment technology, non-equilibrium plasma discharge, is not in thermodynamic equilibrium and only the electron temperature is much hotter than the rest of the gas. Non-equilibrium plasma can generate a reactive environment of heat, ultraviolet (UV) radiation, and highly reactive chemical species such as electrons, ions, and reactive neutral species.[72] At the gas–liquid interface, non-equilibrium plasma generates diverse reactive environments containing a variety of reactive chemical species like reactive oxygen species (ROS, such as $^1O_2$, H_2O_2, O_3, *etc.*), reactive nitrogen species (RNS, such as peroxynitrite, ONOO–, and peroxynitrate, $ONOOO^-$), radicals ($H^\bullet$, $O^\bullet$, $OH^\bullet$, $NO^\bullet$, $NO_2^\bullet$), as well as hydrated electrons (e^-_{aq}).[73–76] These reactive species are responsible for targeting anything dissolved or suspended, including contaminants in the water and potentially degrading them in plasma water treatment system. Plasma water treatment applications can have a multitude of different discharge types, including pulsed corona/streamer/spark discharge, DC pulseless corona discharge, dielectric barrier discharge, gliding arc discharge, DC glow discharge, and DC arc discharge, all leading to different reactive environments with different treatment potentials.[77]

Several studies have investigated the use of non-equilibrium plasma for the treatment of PFAS in water. These publications vary greatly in terms of discharge type, reactor size, degradation efficiencies, length of treatment, and energy costs. There are a number of plasma configurations that produce different types of plasma and reactive species, three of which were demonstrated to degrade PFOA in a study: '7-wires' DC plasma, AC plasma, 'self-pulsing discharge' (SPD) plasma reactor.[78] In this study, they treated 41.4 mg L^{-1} of PFOA in MilliQ water with air plasma with the following results: the '7-wires' DC plasma degraded 12% in 170 mL in 300 minutes, the 'Hollow electrode' AC plasma degraded 49% PFOA in 15 mL in 30 minutes, and the SPD plasma reactor degraded 84% in 15 mL in 30 minutes. Corona pulsed plasma discharged in argon (Ar) gas was demonstrated to degrade PFOA and PFOS in solution to generate carbon dioxide (CO_2) and fluoride (F^-) by generating e^-_{aq}, a reductive process.[67] A follow-up study looked at the byproducts generated for PFOA and PFOS, using the same Ar gas to generate plasma, using a rotating spark gap, and found that PFOA broke down into shorter chain perfluorocarboxylic acids (PFCA) and that PFOS broke down into shorter chain perfluorosulfonic acids (PFSA) as well as shorter chain PFCA,[79] but only accounted for a small fraction of the byproducts generated. Oxygen gas has been shown to be effective in degrading PFOA and PFOS by bubbling oxygen with DC plasma discharge, to produce shorter chain PFCA, taking 3 hours to remove the parent compounds, 41.4 mg L^{-1} PFOA and 8 hours to remove 60 mg L^{-1} PFOS.[80] PFOA and PFOS were able to be removed from solution with plasma jet non-thermal plasma, with air gas being the most effective gas for removal.[81] However, this study used high frequency and power for discharges and had relatively small reactor volumes, 35–45 mL. Investigation-derived waste contaminated with PFAS was treated with plasma and demonstrated removal of PFAS compounds, even at very low concentrations.[82] This group was able to remove 36–99% of the total oxidizable precursor (TOP) concentration present in the investigation derived waste with low energy consumption. Work done investigating the use of non-equilibrium plasma to remove PFAS compounds has demonstrated that it

can be an effective treatment process in laboratory settings, but raises questions on scalability, ability to treat a broad range of PFAS compounds, what byproducts are generated, and amount of energy used.

The objective of this work was to construct a non-equilibrium plasma treatment system for PFAS contaminated liquids that was energy efficient, scalable, fast, and able to destroy a broad range of PFAS compounds, including PFCA, PFSA, and FtS. A promising type of non-equilibrium plasma discharge that is highly energy efficient and readily scalable to industrial levels, is the reverse vortex flow gliding arc plasmatron (GAP).[83,84] The design of the GAP gives possibility to change the reactive environment by altering plasma gas between air, nitrogen and oxygen. In this paper the results from treatment of PFAS in the constructed GAP are presented including the most effective plasma gas for GAP discharge for degradation, the extent of degradation and defluorination for a wide range of PFAS compounds, byproducts generated, and energy use during treatment.

Materials and methods

Chemicals

Table S1 (ESI†) shows the purity, acronyms, formulas, CAS numbers, and manufacturer of the 12 different PFAS used in this study. MilliQ water with a minimum resistance of 18.2 MΩ cm^{-1} was obtained from a Thermo Scientific Barnstead Smart2Pure Water Purification system and used for all analytical analysis. The purity of the N_2 and the O_2 gases were certified to be 99.999% and 99.994%, respectively used in the GAP system. Methanol (purity 99.9%) used in GAP experiments was obtained from Oakwood Products, Inc. (Estill, SC, USA). For RPLC-IC analysis, acetonitrile (purity ≥99.9%), boric acid (purity ≥99.5%) were obtained from Sigma-Aldrich, Co. (St. Louis, MO, USA). Potassium hydroxide, 1N, was obtained from Midland Scientific Inc. (Omaha, NE, USA). Groundwater was obtained from Willow Grove, Pennsylvania, USA. For QTOF analysis methanol and water were LC-MS grade (purity >99%) and purchased from Fisher Scientific (Hampton, NH).

Reverse vortex gliding arc plasmatron (GAP) experiments

A submerged GAP system was used to treat various PFAS in water matrices as seen in Fig. 1. The system was constructed by C&J Nyheim Plasma Institute (Drexel University, Camden, NJ, USA). Plasma gas (compressed air, N_2, or O_2) was injected tangentially in the gap between two cylindrical electrodes. The gliding arc strikes in the gap and plasma gas rotates and stretches the arc with high velocity (1–2 kHz). Portions of the treated water was injected directly from the 1 L reactor into the plasma zone using a water pump and continuously cycled through at a recycle rate of 20 mL min^{-1}.

Solutions of PFAS compounds were prepared by measuring a certain mass or volume of PFAS compound from Table S1 (ESI†) and subsequently adding it to distilled water to achieve the desired concentration in 1 L. Solutions were prepared in polypropylene volumetric flasks to minimize losses due to adsorption processes. To promote dissolution, solutions were then placed on a hot stir plate for two hours before treatment in the GAP system.

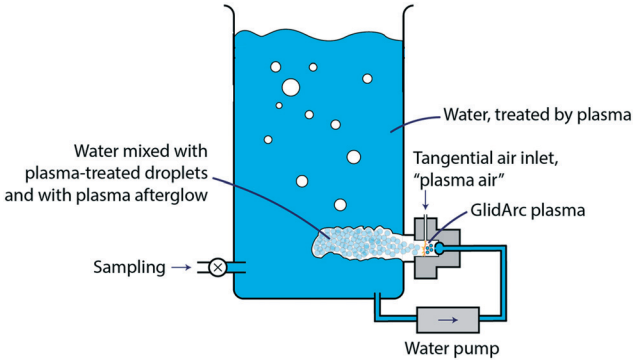


Fig. 1 Schematic of GAP PFAS water treatment system.

Prior to running the prepared solutions in the GAP system, the system was flushed with distilled water. The prepared solution was then loaded into the GAP reactor, gas flow was initiated at a desired flow rate, and the plasmatron power source was turned on, where the current of the power source could be adjusted to tune power settings. Throughout the course of treatment, samples were collected in 15 mL polypropylene vials through the sampling port and stored at 4 °C until analyzed.

Analytical methods

Qualitative UV-vis analysis. To observe chain reduction, a low-cost analytical method was developed using UV-vis analysis.[85] Plasma treated water samples were analyzed using Hitachi Double Beam UV/vis spectrophotometer. To identify species in the treated water, the UV/vis absorption spectra of the water were collected over the wavelengths 200 to 450 nm. The typical UV analysis of water treated by gliding arc discharge are shown in S2 (ESI†). Initial PFOA peak maxima in water correspond to ~214 nm.

RPLC-IC analysis. To quantify PFAS in samples, a modified reverse-phase liquid chromatography – ion chromatograph (RPLC-IC) method was developed for PFAS in water samples.[86] A Shimadzu Prominence HPLC-IC (Shimadzu Scientific Instruments, Columbia, MD) was used to analyze the samples from the GAP experiments for the analytes listed in S1 (ESI†). These analytes had varying ranges of quantification, typically between 100 mg L^{-1} and 0.5 mg L^{-1}. System components include: an autosampler reverse phase column (Acclaim Polar Advantage II, 2.1 × 150 mm, dp = 3 μm, P/N 063187 Dionex, Sunnyvale, CA, USA), a suppressor (Dionex ACRS 500 Chemically Regenerated Suppressor, 2 mm), and an ion conductivity detector (Shimadzu CDD-10Avp, Columbia, MD). Samples were added to 11 mm wide opening polypropylene plastic crimp/snap top vials (Thermo Scientific) and capped with 11 mm silver aluminum crimp caps with polypropylene septum (Thermo Scientific). Polypropylene materials were used to minimize contamination and vial losses.

 This journal is © The Royal Society of Chemistry 2020

To extend lifetime of the analytical column, samples were filtered through a polyethersulfone (PES) 0.22 μm filter to remove polymerized products from treatment and other particles that could affect the column.

Anion analysis for F^-. The concentration of fluoride ions in aqueous samples was measured directly using a fluoride ion selective electrode (Intellical™ ISEF121, Hach, Loveland, CO, USA). This method has a range of 0.01 mg L^{-1} to 19 000 mg L^{-1} F^-, which this experiment was well within. Samples were kept at 4 °C and measurements were taken at room temperature for all standards and samples.

LCMS/MS analysis. For validation of our RPLC/IC analytical method and for analysis of byproducts generated, samples were sent out to Vista Analytical Laboratory (El Dorado Hills, CA, USA), a Department of Defense Environmental Laboratory accredited laboratory. The samples were extracted and analyzed for a selected list of 24 PFAS using Vista Analytical Laboratory (VAL) Method PFAS, a modified EPA Method 537 with a detection limit of 2.0 ng L^{-1}. The results reported for PFHxS, PFOA, PFOS, MeFOSAA, and EtFOSAA include both linear and branched isomers. All other analytes reported include the linear isomers only.

LC-QTOF-MS analysis. PFAS quantitation was performed in HPLC-QTOF-MS (SCIEX x500r QTOF system). LC separation included a delay column (Luna C-18 column, 30 mm long, 3 mm internal diameter) and a analytical column (reverse phase column Gemini C-18, 3 μm particle size, 50 mm length, 3.0 mm internal diameters). Mobile phases were made in LC-MS grade water (phase A) and LC-MS grade methanol (phase B) and included 10 mM ammonium acetate. Analyte separation was achieved by implementing a HPLC gradient method starting at 99% phase A (1% phase B) for 0.5 minute, decreasing to 1% (99% phase B) after 7.5 minutes, and increasing again to 99% phase A (1% phase B) at the end; the entire method duration was 11.5 minutes. Ionization was achieved in negative electrospray ionization (ESI) mode with multiple reaction monitoring (MRM). PFAS were quantified using an 11-point calibration curve (10 ng L^{-1} to 20 μg L^{-1}) and mass-labelled internal standards were used for isotope dilution. Double blanks and quality control vials were also included in the analysis to assess carry-over and identify possible contamination. The limit of quantitation (LOQ) values were analyte specific and spanned 0.01 to 0.1 μg L^{-1} for this method.

Data calculations. Percent destruction was calculated by measuring the initial and final concentration of PFAS in triplicate and dividing average final concentration by average initial concentration. Percent defluorination was calculated by measuring samples initial and final fluoride concentration in triplicate and dividing the final fluoride mass in solution by the mass of fluorine on the initial concentration of PFAS. Energy estimations were calculated by the power setting of the GAP system, time of treatment, and volume of solution treated. Electric energy per order (E_{Eo}) values were calculated in order to compare this technology presented to existing technologies by the formula below. The value represented the energy required (kW h) to degrade a contaminant by an order of magnitude in a unit volume (m^3) of contaminated water.[82,87,88]

$$E_{Eo} = \frac{P \times t \times 1000}{V \times 60 \times \log(C_i/C_f)} \quad (1)$$

Results and discussion

To demonstrate that the engineered GAP system is an effective treatment system for PFAS contaminated water the disappearance of the target analyte(s), formation of degradation products, defluorination, and energy costs were measured and calculated. Examination of only one or a couple of these measurements or calculations is insufficient in evaluating if the destructive method of PFAS is a beneficial or effective method. As a result, the data needs to be co-aligned to show that PFAS are truly destroyed and not just altered, in an energy efficient way shown in the following sections.

Effectiveness of different plasma gasses on PFAS degradation in GAP system

The reactive environment created by plasma can be altered by the type of discharges generated in the reactor. The reactive species produced from non-equilibrium plasma can be tuned by changing the gas used and the type of plasma discharge.[72] Since the GAP system was designed for generating reverse-vortex gliding arc discharges, air, nitrogen (N_2), and oxygen (O_2) were compared to determine which gas leads to the most rapid degradation of PFAS compounds in aqueous matrices. The most effective plasma gas was determined by comparing the percent destruction of PFNA, PFOS, and 8 : 2 FtS (each, respectively, a PFCA, PFSA, and FtS compound with eight perfluoroalkyl carbons chain). It was found that air achieved the most rapid destruction for the three compounds test, with 96.9% of PFNA, 93.1% of PFOS, and 99.7% of 8 : 2 FtS destroyed in 1 hour of treatment (Fig. 2).

Atmospheric air contains mainly nitrogen and oxygen as the main gaseous species by volume. Since nitrogen and oxygen gas were less effective than air for destruction of the three PFAS compounds tested, it suggests that the mechanism responsible could involve both ROS and RNS. Because air is mainly oxygen and nitrogen, ROS, RNS, and radicals are expected to be generated by non-equilibrium plasma.[74] Although electrons are produced in air plasma sources, the electronegative O_2 molecules in the gas rapidly react with the electrons and reduce the electron flux to solution.[89] Even if electrons make it to the liquid as e^-_{aq}, they are quickly scavenged by RNS in the liquid, including NO_3^- and NO_2^-, which are also produced by air plasmas. In addition to these reactive species generated, UV and visible radiation and thermal energy are can also play a role in degradation processes in non-equilibrium air plasmas.[79,90,91] Since the half-lives of the ROS, RNS, and radicals generated in air plasma are highly temperature sensitive,[92,93] the system temperature can play a role in the reactive species formed in the GAP system.

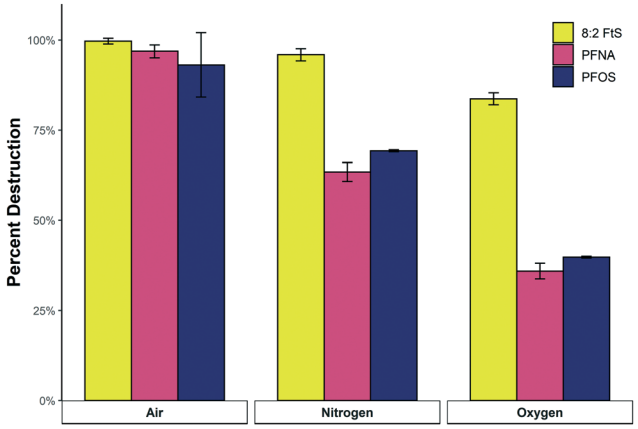


Fig. 2 Effect of gas used for plasma discharge on destruction of PFNA, PFOS, and 8 : 2 FtS. Experimental conditions: ~100 mg L^{-1} PFAS, 50 L min^{-1} gas flow, 150 W power output setting, 1 hour treatment time. Concentrations reported were determined by RPLC-IC method. Error bars represents standard deviation values (n = 6 for all data points besides PFOS treatment with air as a plasma source (n = 18)).

Another study investigating non-equilibrium plasma generated with air for treatment of PFAS contaminated solutions, which instead used a PlasmaBeam®, also found air to be more effective than N_2 and O_2.[81] While the PlasmaBeam® and the GAP reactor used in this study both produce forms of gliding arc discharges, the mixing characteristics of the gas flow and the electronics of the plasma source can have an impact on the reactive environments generated in each system. For example, the reactor using PlasmaBeam® used a smaller gas flow rate. Additionally, the GAP system uses a reverse flow vertex gliding arc gas flow design.[84] As demonstrated in a similar study using air as the plasma feed gas but a different plasma discharge,[78] some amount of nitrogen containing species in the liquid phase (such as nitrous acid and nitric acid) and ozone and nitric oxide in the gaseous phase are likely byproducts of the GAP treatment system.

Air plasma as an effective treatment of contaminated water with PFCA, PFSA, and FtS

Although PFOS and PFOA are frequently found and reported to be in the environment at contaminated sites with historical use of AFFF, a wider range of PFAS are present and have been detected, including PFCA, PFSA, and FtS.[22,23,94–96] While PFCA, PFSA, and FtS compounds all have the characteristic perfluorinated carbon chain, they have differences in their head group, leading to different transport processes in the environment, abilities to degrade, and toxicity in biological settings. To date, non-equilibrium plasma discharges have been demonstrated to remove PFOS and PFOA dissolved in water,[67,80,81] with one other study reporting the degradation of short- and long-chain perfluoroalkyl acids (PFAA), FtS, and precursor compounds in investigation derived wastes by argon plasma.[97] Fig. 3 demonstrates the ability of gliding arc plasma discharge to destroy 12 different PFCA, PFSA, and FtS compounds of differing carbon chain lengths within the GAP reactor. All compounds were evaluated individually and had an initial concentration of ~100 mg L^{-1} in MilliQ water and were treated at 150 W power output settings, 50 L min^{-1} air flow, and for 1 hour of treatment time. Longer chain PFAS were observed to be destroyed more quickly in the reactor than shorter chain compounds. While there are many reactive species present in the bulk liquid, most of the destruction of PFAS happens at the air–water interface, or the plasma interface. Reactive species present in the bulk liquid can attack the head group of FtS and PFSA compounds, converting them to carboxylates. PFOS degradation in plasma treatment systems has been proposed to be slower because of the sulfonate head group.[98] They proposed that PFOS breaks down to PFOA first through desulfonation, and then must follow the same chain length reduction mechanism, which is responsible for the delay. PFAS reduction by non-equilibrium plasma has also been proposed to occur by shortening of the chain length from side of the head group in a step-wise reaction, while producing CO_2 and removing one carbon from the chain length.[99] The results reported in this manuscript and in another publication[82] demonstrate that plasma treatment is more effective for sulfonates so the mechanisms could vary between types of plasma treatment and is not fully understood.

In the GAP system presented in this paper, the flow rate of gas is very high resulting in thorough mixing of reactive species and PFAS contaminated water. Since PFOA and other PFAS adsorb to the gas–water interface,[67] most of its hydrophobic tail extends into the gas phase where thermal decomposition or reactions with gas phase electrons and ions can occur, even in non-equilibrium plasma treatment systems. Fig. 2 and 3 demonstrates compounds with identical

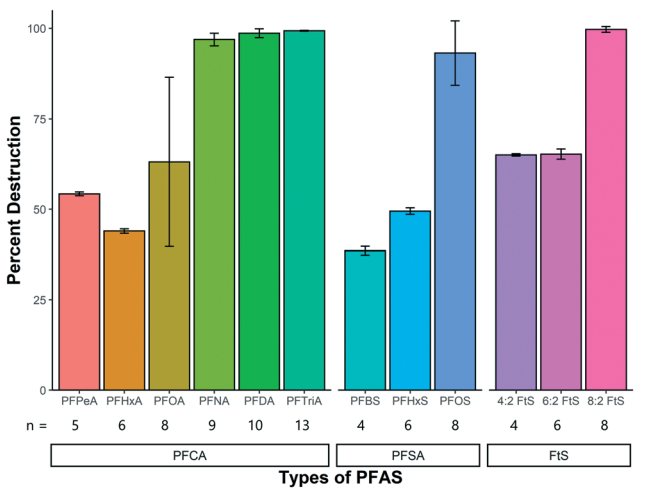


Fig. 3 Percent destruction of PFCA, PFSA, FtS as a function of chain length (C_nF_{n+1}). Experimental conditions: ~100 mg L^{-1}, 50 L min^{-1} air flow, 150 W power output setting, 1 hour of treatment time. Concentrations reported were measured using RPLC-IC method. Error bars represents standard deviation values (n = 6 for all data points besides PFOS and PFOA (n = 18)).

This journal is © The Royal Society of Chemistry 2020

perfluoroalkyl chain lengths (PFNA, PFOS, and 8 : 2 FtS) have similar amounts of removal and defluorination. This suggests that most of the degradation mechanisms in the GAP system relates to reduction of the fluorinated chain from the hydrophobic end, in addition to some transformation of the head group from reactive species in the bulk liquid. It is observed from the data that the FtS compounds with similar perfluorinated chain lengths to PFSA (*e.g.*, PFBS and 4 : 2 FtS; PFHxS and 6 : 2 FtS; PFOS, and 8 : 2 FtS) were destroyed more within an hour (Fig. 3), demonstrating that the methyl groups in the telomeric portion of FtS compounds could be attacked by reactive species in the bulk liquid.

Characterization of degradation products in treatment system: evidence of chain reduction, defluorination, and byproducts generated

While it is promising that a range of PFCA, PFSA, and FtS compounds can be rapidly destroyed in the GAP system constructed (Fig. 2 and 3), it is important to examine the degradation products generated throughout the treatment process because they are also a concern in the environment. In this study, qualitative UV-vis analysis was used to look at chain reduction, LCMS/MS and QTOF were used to look at byproduct PFAS compounds, and defluorination was measured using a fluorine selective probe.

The UV-vis analysis was conducted to qualitatively observe chain reduction of PFCAs. For PFCAs, the wavelength and intensity for maximal UV absorption decreases as the carbon chain length increases.[85] Therefore, UV-vis can be used to assess chain length reduction. For example, for degradation of PFOA, initial peak maxima in water corresponded to ~214 nm and was observed to shift towards longer wavelengths during the treatment process, as seen in S2 (ESI†).

Defluorination was measured by a fluorine selective ion-probe for the PFCA, PFSA, and FtS compounds tested (Fig. 4). A trend of greater defluorination was observed in the longer chain lengths than the shorter chain lengths. Defluorination of PFAS chemicals is significant since mineralization of these compounds is the goal. Longer treatment times result in greater magnitudes of defluorination in addition to reduction in chain length and removal of head group. Since the C–F bond is very recalcitrant, especially once it is found in environmental settings, a strong focus on complete mineralization of these compounds is a priority. In order to measure the progress throughout treatment of mineralization, defluorination was measured for different time points (S4, ESI†). It was observed that percent destruction of compounds over time was greatly reduced, but defluorination occurred at a much slower pace due to the strength of the C–F bonds.

Although the parent compounds being tested were substantially removed during treatment in the GAP reactor and UV-vis analysis indicated chain length reduction was occurring, it is important to determine what byproducts are generated. From LC-MS/MS and QTOF analyses, measurement of changes in a number of quantifiable PFAS byproducts were observed during degradation of PFOA, PFOS, and 8 : 2 FtS by non-thermal air plasma. During the treatment of PFOA (Fig. 5(A)), a PFCA, the concentration of shorter chain PFCA, such as PFBA, PFHxA, and PFHpA increased. This suggests that the longer chain of PFOA is shortened throughout treatment however the mechanism for chain reduction is unknown. Similarly, during the treatment of PFOS (Fig. 5(B)), a PFSA, the concentrations of shorter chain PFCA increased, while the concentration of PFSA (as impurities) decreased over treatment time. During the treatment of the mixed system (S3(d), ESI†), the concentrations of PFCA and PFSA decreased overtime except for PFOS. While there is significant evidence of perfluoroalkyl chain length reduction, it also appears that the head groups of the PFAS tested can be cleaved during treatment in the GAP reactor. For example, in the batch experiments with PFOS and 8 : 2 FtS (Fig. 5(B) and S3†), the formation of PFOA in the treatment of PFOS and the formation of PFOS in the treatment of 8 : 2 FtS were observed.

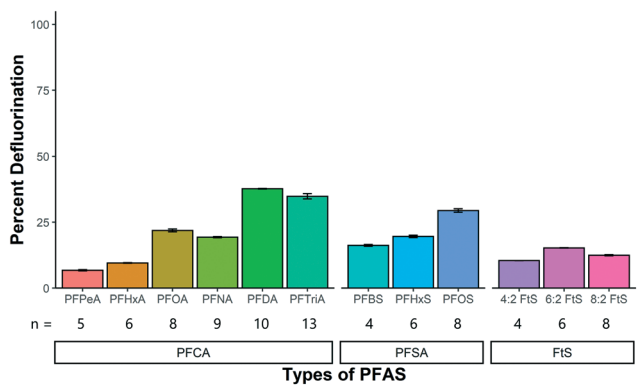


Fig. 4 Percent defluorination of PFCA, PFSA, FtS as a function of chain length (C_nF_{n+1}). Experimental conditions: ~100 mg L^{-1} PFAS, 50 L min^{-1} air flow, 150 W power output setting, 1 hour of treatment time. Error bars represents standard deviation values (n = 6 for all data points).

Fluorine mass balance for treatment of PFAS in GAP system

The C–F bond in PFAS compounds is recalcitrant to degradation, so it is important to look at where the fluorine ends up during the course of destructive treatments. In Fig. 6 fluorine was tracked on the initial analyte being tested, the quantifiable byproduct/co-contaminant fluorine measured by the LC-MS/MS method, and fluoride. Fig. 6 demonstrates all of the analytical measurements taken and the accounting of total fluorine in the sample. From this accounting, it is apparent that the amount of the parent compound converted to other quantifiable PFCA, PFSA or FTS compounds was significantly low. For example, in Fig. 6(A), even though concentration of PFOA dropped from 70 100 μg L^{-1} to 52 800 μg L^{-1} the concentration of any quantifiable PFAS byproducts/co-contaminants were below 500 μg L^{-1} (less than 3% of the amount of PFOA converted). This suggests that when a PFCA is degraded within the reactive environment, it is mineralized completely

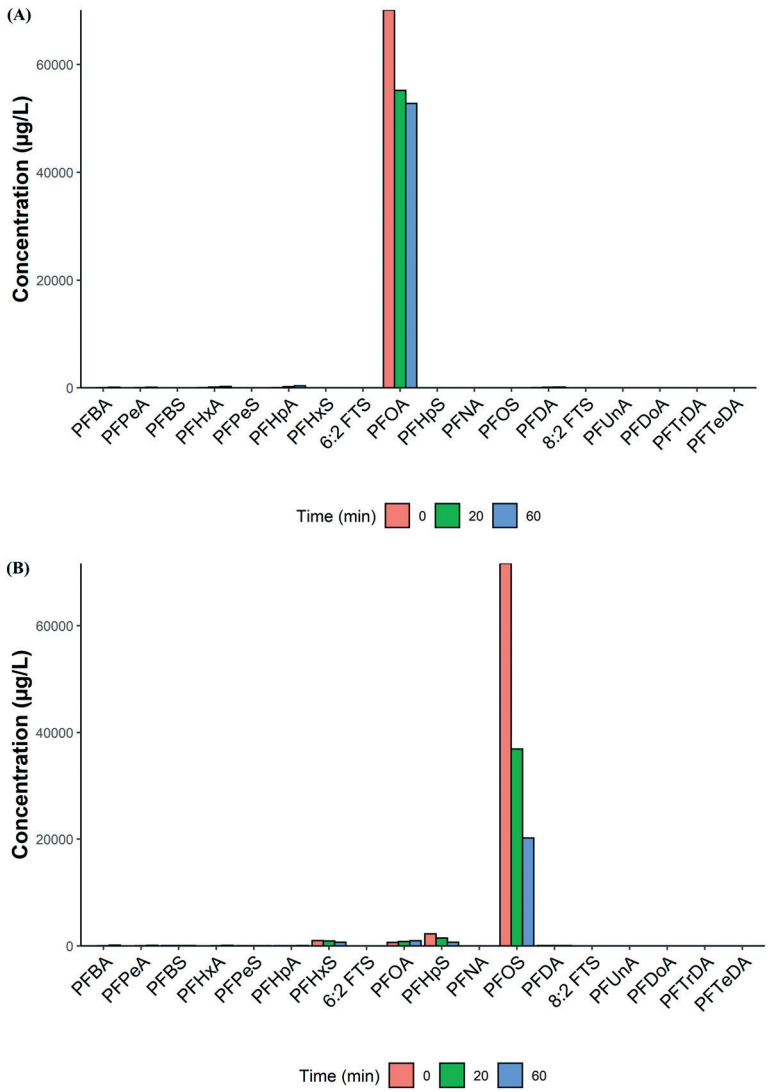


Fig. 5 Byproducts generated during treatment of (A) PFOA, (B) PFOS in the GAP reactor in MilliQ water. Experimental conditions: 50 L min^{-1} air flow, 150 W power setting, 1 hour of treatment. Concentrations presented were determined *via* the LC-MS/MS method. All analytes by the LC-MS/MS method were measured as described, but compounds not found were removed from this figure.

to CO_2 and F^-. However, when the PFAS compound is not a PFCA, tracking of the total fluorine is more complicated as seen in Fig. 6(B) and S5 (ESI†). If the PFAS being tested has its head group altered or is partially or complete defluorinated, it can no longer be detected by the methods used in this paper and could form non-quantifiable byproducts. Additionally, there could be more volatilization and adsorption of the byproducts in the system, preventing a full closure of the fluorine mass balance. Further investigations are needed to close the mass balance on more complicated PFAS compounds in the GAP reactor.

Matrix and potential co-contaminant effects on PFAS compound removal

PFAS solutions prepared in MilliQ water can demonstrate the mechanisms of destruction and byproducts generated but are not representative of PFAS contaminated water in the environment of water treatment systems. It is important to look at the effectiveness of the GAP treatment system on environmental matrices, such as groundwater. Groundwater was spiked individually with 8 : 2 FtS, PFOA, and PFOS and the percent destruction for the spiked groundwater and spiked distilled water were compared to see the ability to treat contaminated environmental solutions (Fig. 7). It was demonstrated that these compounds could be destroyed in natural waters, not just distilled water, by spiking collected groundwater with PFAS, but it had about an hour delay to reach the same removal. Organic compounds, salts, and other organic matter in groundwater samples can interfere with the effectiveness of plasma treatment of water and have an inhibitory effect but was shown to not have too great of an effect in the GAP system. Additionally, PFAS spiked MilliQ had methanol added to it (S6, ESI†) to

 This journal is © The Royal Society of Chemistry 2020

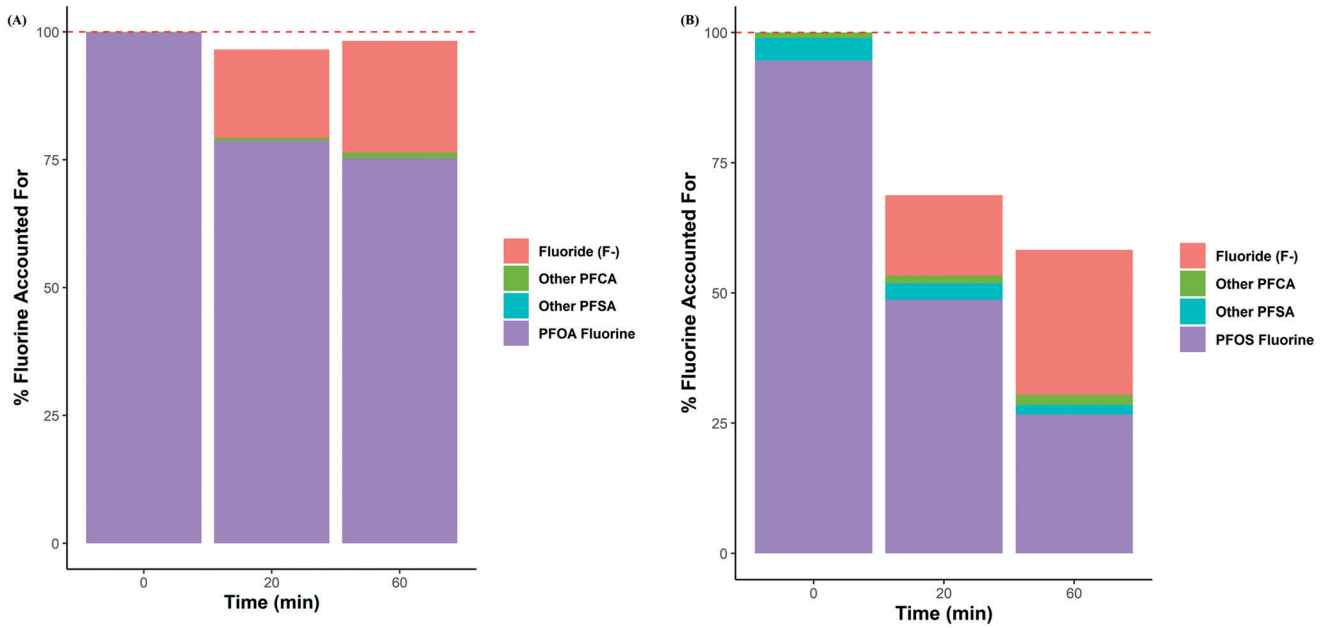


Fig. 6 Fluorine mass balances of (A) PFOA and (B) PFOS. PFAS and other quantifiable PFAS (broken down into PFCA, PFSA, and FtS) were measured using LC-MS/MS method. Fluoride was measured using the fluoride selective probe. All measurements were taken from samples from a single experimental run.

observe the effect of solely organics in the water, demonstrating little to no effect on removal efficiency.

Estimated energy cost of PFAS removal

The GAP treatment system developed has demonstrated ability to destroy a wide range of PFAS compounds rapidly and can be scaled to treat large volumes of water. In addition to its promise in scalability[100,101] and effectiveness in removal of PFAS, it is important to demonstrate that GAP treatment can be a relatively low energy process. Since altering the power setting of the GAP can potentially affect the reactive environment generated, different power settings were tested to assess their impact on treatment of PFOA and PFOS (S7, ESI†) and from this data determine the amount of energy required to achieve a certain degree of removal, which can be calculated by multiplying the time elapsed by the power setting and dividing by the total volume of the reactor and plotting the corresponding degree of destruction achieved over that duration (Fig. 8). From these experiments, it can be seen that the plasma power settings that led to the greatest percent destruction in one hour was at 180 W for PFOS (180b in Fig. 8) and at 255 W for PFOA. In addition, for the majority of the different power settings tested (Fig. 8), it was demonstrated from these calculations (Fig. 8) that to achieve progressively higher degrees of removal that the amount of energy required increases (*i.e.*, the slope for each experimental curve increases as percent destruction increases). It is important to note that for the experiment with no power but with the same gas flow (see S6 (ESI†)) that adsorption of PFAS to the reactor or other losses were not a significant mechanism for removal in the system.

In order to determine the most energy efficient cost for destruction of PFAS in water by GAP from the experimental data, one has to identify the shallowest slope observed in Fig. 8. For PFOA (Fig. 8(A)), this occurs for the experiment ran at 140 W. For this experiment, the most energy efficient removal achieved was 21% destruction and 17% defluorination in 20 minutes at 150 W (Fig. 3 and 4). This regime of near complete mineralization of the amount PFOA degraded in 20 minutes corresponds to 180 kJ L^{-1} of energy used. If this energy efficiency could have been maintained, it would require 900 kJ L^{-1} of energy to completely degrade PFOA. However, due to reactor inefficiencies of the current GAP reactor design, the highest amount of removal achieved was 75% and required 918 kJ L^{-1} at a power setting of 255 W (Fig. 8). For PFOS, the most energy efficient removal was observed at 180 W (see 180b curve in Fig. 8), where 25% destruction was achieved in 1 minute, corresponding to 10.8 kJ L^{-1}. If this energy efficient could have been maintained, it would require 54 kJ L^{-1} of energy to completely degrade PFOS. However, due to reactor inefficiencies, it required approximately 625 kJ L^{-1} to achieve a maximum of 90% removal.

For comparison to other treatment technologies for PFAS contaminated water, electric energy per order (E_{Eo}) was calculated. The lowest values measured in the GAP reactor was 23.2 kW h m^{-3} per order for PFOS and 213.4 kW h m^{-3} per order for PFOA. Even though the GAP reactor presented is not optimized it is still on par with other technologies,[88] but on an order of magnitude higher than a study using rotating spark gap discharge with argon gas.[82]

These reactor inefficiencies are likely due to the low recycle rate (20 mL min^{-1}) of the water that directly passes by the

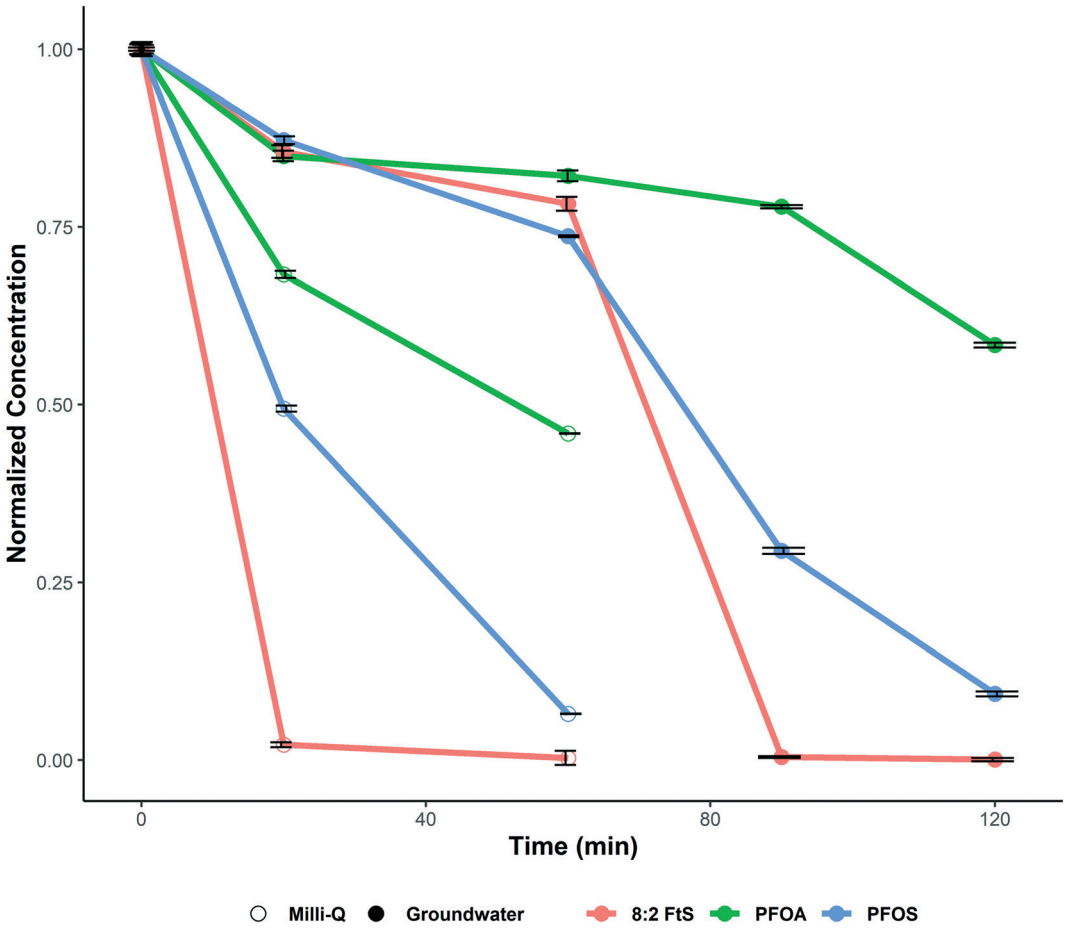


Fig. 7 Treatment of groundwater or Milli-Q water spiked with 8 : 2 FtS, PFOA, and PFOS over time. Experimental conditions: ~100 mg L^{-1} PFAS, 50 L min^{-1} air flow, 150 W power output setting, varying treatment times. Concentrations reported were measured by LC-MS/MS method. Error bars represents standard deviation values (n = 3 for all data points).

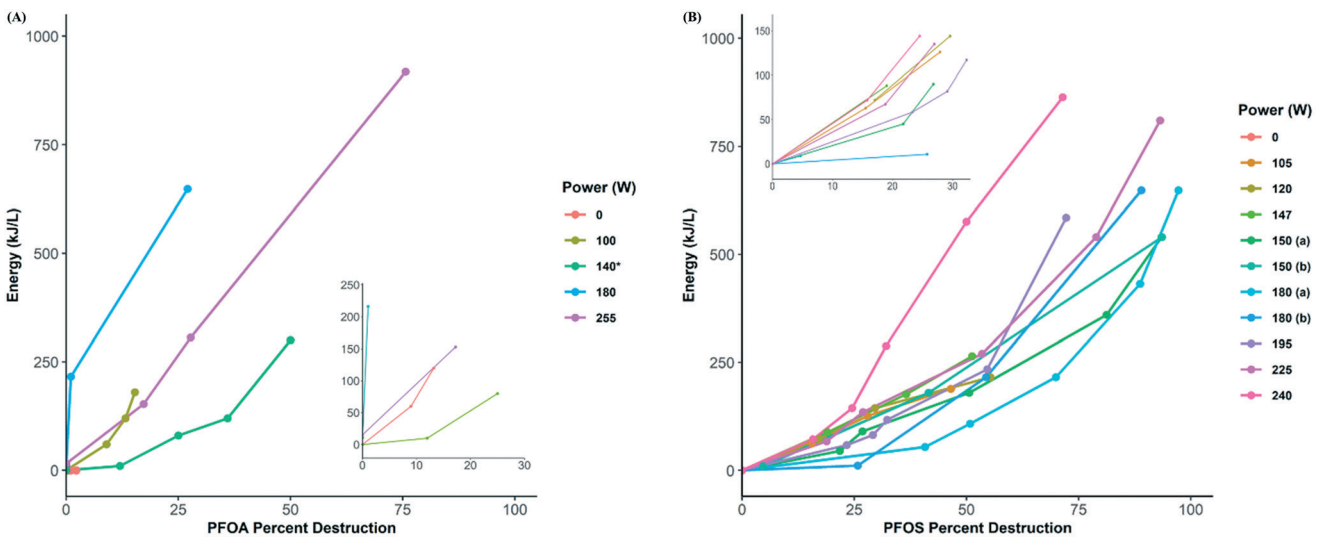


Fig. 8 Percent destruction of (A) PFOA and (B) PFOS by energy consumed. Experimental conditions: 50 L min^{-1} air, varying treatment times and power settings. Concentrations reported were measured by RPLC-IC method. Fig. 8(A) "140*" concentrations were measured by UV–vis method. Inset graphs show greater resolution of the data at lowest energy usages.

plasmatron for the 1 L GAP reactor used for this study. Despite the inefficiencies, which should be overcome with future improvements to reactor design of the GAP system, the results in the paper demonstrate that PFAS can be

 This journal is © The Royal Society of Chemistry 2020

degraded by non-equilibrium plasma at relatively low energies (*e.g.*, the amount of energy to evaporate water is approximately 3000 kJ L^{-1}).

Conclusions

The novel H_2O submerged cold gliding arc plasma stabilized in reverse vortex demonstrated high efficiency of PFAS removal from contaminated water. Advantages of the GAP system for PFAS removal are that non-equilibrium provides high flux of atoms, radicals and other active plasma species that significantly decrease activation barriers of PFAS destruction, has significant bubbling and increased plasma–water surface contact area, little formation of shorter chain PFAS, and is very scalable. While the results are promising from this study, future optimization of the system is needed to ensure that this form of non-equilibrium plasma can be developed to achieve complete destruction of PFAS (*i.e.*, mineralization) at lower energy costs and at more environmentally relevant concentrations.

Conflicts of interest

There are no conflicts of interest to declare.

Acknowledgements

This work was funded through SERDP grant (ER18-1570).

References

1 E. Kissa, *Fluorinated surfactants and repellents*, CRC Press, Boca Raton, FL, 2nd edn, 2001.
2 J. M. Conder, R. A. Hoke, W. de Wolf, M. H. Russell and R. C. Buck, Are PFCAs bioaccumulative? A critical review and comparison with regulatory lipophilic compounds, *Environ. Sci. Technol.*, 2008, **42**(4), 995–1003.
3 E. D. Olsen, *Perfluorinated Chemicals in the Environment: An Update on the Response to Contamination and Challenges Presented. Sect. United States House of Representatives Committe on Energy and Commerce Subcommittee on Environment*, 2018.
4 K. E. Boronow, J. G. Brody, L. A. Schaider, G. F. Peaslee, L. Havas and B. A. Cohn, Serum concentrations of PFASs and exposure-related behaviours in African American and non-Hispanic white women, *J. Exposure Sci. Environ. Epidemiol.*, 2019, **29**, 206–217.
5 S. Fujii, C. Polprasert, S. Tanaka, N. P. H. Lien and Y. Qui, New POPs in the water environment: Distribution, bioaccumulation and treatment of perfluorinated compounds - A review paper, *J. Water Supply: Res. Technol.–AQUA*, 2007, **56**(5), 313–326.
6 E. F. Houtz, C. P. Higgins, J. A. Field and D. L. Sedlak, Persistence of perfluoroalkyl acid precursors in AFFF-impacted groundwater and soil, *Environ. Sci. Technol.*, 2013, **47**(15), 8187–8195.
7 K. Prevedouros, I. T. Cousins, R. C. Buck and S. H. Korzeniowski, Sources, fate, and transport of perfluorocarboxylates, *Environ. Sci. Technol.*, 2006, **40**(1), 32–44.
8 M. Sun, E. Arevalo, M. Strynar, A. Lindstrom, M. RIchardson and B. Kearns, *et al.* Legacy and emergying perfluoroalkyl substances are important drinking water contaminants in the Cape Fear River Watershed of North Carolina, *Environ. Sci. Technol. Lett.*, 2016, **3**(12), 415–419.
9 P. Rostkowski, N. Yamashita, I. M. K. So, S. Taniyasu, P. K. S. Lam and J. Falandysz, *et al.* Perfluorinated compounds in streams of the Shihwa industrial zone and Lake Shihwa, South Korea, *Environ. Toxicol. Chem.*, 2006, **25**(6), 2374–2380.
10 H. Chen, C. Zhang, J. Han, R. Sun, X. Kong and X. Wang, *et al.* Levels and spatial distribution of perfluoroalkyl substances in China Liaodong Bay basin with concentrated fluorine industry parks, *Mar. Pollut. Bull.*, 2015, **101**(2), 965–971.
11 R. Kim Lazcano, C. de Perre, M. L. Mashtare and L. S. Lee, Per- and polyfluoroalkyl substances in commercially available biosolid-based products: The effect of treatment process, *Water Environ. Res.*, 2019, **91**(12), 1669–1677.
12 A. K. Venkatesan and R. U. Halden, National inventory of perfluoroalkyl substances in archived US biosolids from the 2001 EPA National Sewage Sledge Survey, *J. Hazard. Mater.*, 2013, **252**, 413–418.
13 C. Gallen, G. Eaglesham, D. Drage, T. Hue Nguyen and J. F. Mueller, A mass estimate of perfluoroalkyl substance (PFAS) release from Australian wastewater treatment plants, *Chemosphere*, 2018, **208**, 975–983.
14 J. R. Lang, B. M. Allred, J. A. Field, J. W. Levis and M. A. Barlaz, National estimate of per- and polyfluoroalkyl substances (PFAS) release to US municipal landfill leachate, *Environ. Sci. Technol.*, 2017, **51**(4), 2197–2205.
15 Z. Wei, T. Xu and D. Zhao, Treatment of per- and polyfluoroalkyl substances (PFAS) release to US municipal landfill leachate, *Environ. Sci.: Water Res. Technol.*, 2019, **51**(4), 2197–2205.
16 N. Perkola and P. Sainio, Survey of perfluorinated alkyl acids in Finnish effluents, storm water, landfill leachate and sludge, *Environ. Sci. Pollut. Res.*, 2013, **20**(11), 7979–7987.
17 I. Fuertes, S. Gómez-Lavín, M. Elizalde and A. Urtiaga, Perfluorinated alkyl substances (PFASs) in northern Spain municipal solid waste landfill leachates, *Chemosphere*, 2017, **168**, 399–407.
18 W. Zhang, Y. Zhang, S. Taniyasu, L. W. Yeung, P. K. Lam and J. Wang, *et al.* Distribution and fate of perfluoroalkyl substances in municipal wastewater treatment plants in economically developed areas of China, *Environ. Pollut.*, 2013, **176**, 10–17.
19 H. Hamid and L. Y. Li, Role of wastewater treatment plant in environmental cycling of poly- and perfluoroalkyl substances, *Ecocycles*, 2016, **2**(2), 43–53.
20 H. Chen, C. Zhang, J. Han, Y. Yu and P. Zhang, PFOS and PFOA in influents, effluents, and biosolids of Chinese

wastewater treatment plants and effluent-receiving marine environments, *Environ. Pollut.*, 2012, **170**, 26–31.

21 M. F. Rahman, S. Peldszuz and W. B. Anderson, Behaviour and fate of perfluoroalkyl and polyfluoroalkyl substances (PFASs) in drinking water treatment: A review, *Water Res.*, 2014, **50**, 318–340.

22 W. J. Backe, T. C. Day and J. A. Field, Zwitterionic, cationic, and anionic fluorinated chemicals in aqueous film forming foam formulations and groundwater from US military bases by nonaqueous large-volume injection HPLC-MS/MS, *Environ. Sci. Technol.*, 2013, **47**(10), 5226–5234.

23 X. Dauchy, V. Boiteux, A. Colin, C. Bach, C. Rosin and J. F. Munoz, Poly- and perfluoroalkyl substances in runoff water and wastewater sampled at a firefighting training area, *Arch. Environ. Contam. Toxicol.*, 2019, **76**(2), 206–215.

24 X. C. Hu, D. Q. Andrews, A. B. Lindstrom, T. A. Bruton, L. A. Schaider and P. Grandjean, *et al.* Detection of poly- and per-fluoroalkyl substances (PFASs) in U.S. drinking water linked to industrial sites, military fire training areas, and wastewater treatment plans, *Environ. Sci. Technol. Lett.*, 2016, **3**(10), 344–350.

25 F. Xiao, Emerging poly- and perfluoroalkyl substances in the aquatic environment: A review of current literatures, *Water Res.*, 2017, **124**, 482–495.

26 V. Gellrich, T. Stahl and T. Knepper, Behavior of perfluorinated compounds in soils during leaching experiments, *Chemosphere*, 2012, **87**(9), 1052–1056.

27 H. Shin, V. Vieira, P. Ryan, R. Detwiler, B. Sanders and K. Steenland, *et al.* Environmental fate and transport modeling for perfluorooctanoic acid emitted from the Washington Works Facility in West Virginia, *Environ. Sci. Technol.*, 2011, **45**(4), 1435–1442.

28 R. Hunter Anderson, G. Cornell Long, R. C. Porter and J. K. Anderson, Occurence of select perfluoroalkyl substances at U.S. Air Force aqueous film-forming foam release sites other than fire-training areas: Field-validation of critical fate and transport properties, *Chemosphere*, 2016, **150**, 678–685.

29 M. Brusseau, N. Yan, S. van Glubt, Y. Wang, W. Chen and Y. Lyu, *et al.* Comprehensive retention model for PFAS transport in subsurface systems, *Water Res.*, 2019, **148**, 41–50.

30 N. Wang, B. Szostek, R. C. Buck, P. W. Folsom, L. M. Sulecki and V. Capka, *et al.* Fluorotelomer alcohol biodegradation - direct evidence that perfluorinated carbon chains breakdown, *Environ. Sci. Technol.*, 2005, **39**(19), 7516–7528.

31 S. Wild, D. McLagen, M. Schlabach, R. Bossi, D. Hawker and R. Cropp, *et al.* An Antarctic research station as a source of brominated and perfluorinated persistent organic pollutants to the local environment, *Environ. Sci. Technol.*, 2014, **49**(1), 103–112.

32 F. M. Hekster, R. W. Laane and P. de Voogt, Environmental and toxicity effects of perfluoroalkylated substances, *Rev. Environ. Contam. Toxicol.*, 2003, 99–121.

33 F. Suja, B. K. Pramanik and S. M. Zain, Contamination, bioaccumulation and toxic effects of perfluorinated chemicals (PFCs) in the water environment: a review paper, *Water Sci. Technol.*, 2009, **60**(6), 1533–1544.

34 E. M. Sunderland, X. C. Hu, C. Dassuncao, A. K. Tokranov and C. C. Wagner, A review of the pathways of human exposure to poly- and perfluoroalkyl substances (PFASs) and present understanding of health effects, *J. Exposure Sci. Environ. Epidemiol.*, 2019, **29**, 131–147.

35 V. Barry, A. Winquist and K. Steenland, Perfluorooctanoic acid (PFOA) exposures and incident cancers among adults living near a chemical plant, *Environ. Health Perspect.*, 2013, **121**(11–12), 1313–1318.

36 M. Lopez-Espinosa, D. Mondal, B. Armstrong, M. Bloom and T. Fletcher, Thyroid function and perfluoroalkyl acids in children living near a chemical plant, *Environ. Health Perspect.*, 2012, **120**(7), 1036–1041.

37 K. Steenland, L. Zhao, A. Winquist and C. Parks, Ulcerative colitis and perfluoroocatanoic (PFOA) in a highly exposed population of community residents and workers in the mid-Ohio valley, *Environ. Health Perspect.*, 2013, **121**(8), 900–905.

38 L. Darrow, C. Stein and K. Steenland, Serum perfluorooctanoic acid and perfluorooctane sulfonate concentrations in relation to birth outcomes in the Mid-Ohio Valley, 2005-2010, *Environ. Health Perspect.*, 2013, **121**(10), 1207–1213.

39 D. Parson, T. Duignan and A. Salis, Cation effects on haemoglobin aggregation: balance of chemisorption against physisoprtion of ions, *Interface Focus*, 2017, **7**(4), 20160137.

40 X.-M. Ren, W.-P. Qin, L.-Y. Cao, J. Zhang, Y. Yang and B. Wan, *et al.* Binding interactions of perfluoroalkyl substances with thyroid hormone transport proteins and potential toxicological implications, *Toxicology*, 2016, **366–367**, 32–42.

41 P. McCleaf, S. Englund, A. Östlund, K. Lindegren and K. Wiberg, Removal efficiency of multiple poly- and perfluoroalkyl substances (PFASs) in drinking water using granular activated carbon (GAC) and anion exchange (AE) column tests, *Water Res.*, 2017, **120**, 77–87.

42 V. Ochoa-Herrera and R. Sierra-Alvarez, Removal of perfluorinated surfactants by sorption onto granular activated carbon, zeolite and sludge, *Chemosphere*, 2008, **72**(10), 1588–1593.

43 A. Zaggia, L. Conte, L. Falletti, M. Fant and A. Chiorboli, Use of strong anion exchange resin for the removal of perfluoroalkylated substances from contaminated drinking water in batch and continuous pilot plants, *Water Res.*, 2016, **91**, 137–146.

44 S. Woodard, J. Berry and B. Newman, Ion exchange resin for PFAS removal and pilot test comparison to GAC, *Rem. J.*, 2017, **27**(3), 19–27.

45 M. J. Klemes, Y. Ling, C. Ching, C. Wu, L. Xiao and P. D. E. Helbling, *et al.* Reduction of a tetrafluoroterephthalonitrile-β-cyclodextrin polymer to remove anionic micropollutants and perfluorinated alkyl substances from water, *Angew. Chem., Int. Ed.*, 2019, **58**, 12049–12053.

 This journal is © The Royal Society of Chemistry 2020

46 B. D. Turner, S. W. Sloan and G. R. Currell, Novel remediation of per-and polyfluoroalkyl substances (PFASs) from contaminated groundwater ussing Cannabis Sativa L. (hemp) protein powder, *Chemosphere*, 2019, **229**, 22–31.

47 N. A. Fernandez, L. Rodriguez-Freire, M. Keswani and R. Sierra-Alvarez, Effect of chemical structure on the sonochemical degradation of perfluoroalkyl and polyfluoroalkyl substances (PFASs), *Environ. Sci.: Water Res. Technol.*, 2016, **2**, 975–983.

48 T. Shende, G. Andaluri and R. P. Suri, Kinetic model for sonolytic degradation of non-volatile surfactants: Perfluoroalkyl substances, *Ultrason. Sonochem.*, 2019, **51**, 359–368.

49 C. D. Vecitis, Y. Wang, J. Cheng, H. Park, B. T. Mader and M. R. Hoffmann, Sonochemical degradation of perfluorooctanesulfonate in aqueous film-forming foams, *Environ. Sci. Technol.*, 2010, **44**, 432–438.

50 V. L. Gole, A. Fishgold, R. Sierra-Alvarez, P. Deymier and M. Keswani, Treatment of perfluorooctane sulfonic acid (PFOS) using a large-scale sonochemical reactor, *Sep. Purif. Technol.*, 2018, **193**, 104–110.

51 C. Liu, C. Higgins, F. Wang and K. Shih, Effect of temperature on oxidative transformation of perfluorooctanoic acid (PFOA) by persulfate activation in water, *Sep. Purif. Technol.*, 2012, **91**, 46–51.

52 J. Huang, X. Wang, Z. Pan, X. Li, Y. Ling and L. Li, Efficient degradation of perfluorooctanic acid (PFOA) by photocatalytic ozonation, *Chem. Eng. J.*, 2016, **296**, 329–334.

53 Q. Zhuo, S. Deng, B. Yang, J. Huang and G. Yu, Efficient electrochemical oxidation of perfluorooctanoate using a Ti/SnO2-Sb-Bi anode, *Environ. Sci. Technol.*, 2011, **45**(7), 2973–2979.

54 C. E. Schaefer, C. Andaya, A. Urtiaga, E. R. McKenzie and C. P. Higgins, Electrochemical treatment of perfluorooctanoic acid (PFOA) and perfluorooctane sulfonic acid (PFOS) in groundwater impacted by aqueous film forming foams (AFFFs), *J. Hazard. Mater.*, 2015, **295**, 170–175.

55 C. E. Schaefer, C. Andaya, A. Burant, C. W. Condee, A. Urtiaga and T. J. Strathmann, *et al.* Electrochemical treatment of perfluorooctanoic acid and perfluorooctane sulfonate: Insights into mechasisms and application to groundwater treatment, *Chem. Eng. J.*, 2017, **317**, 424–432.

56 G. Niu, W. Li, F. Meng, L. Wang, H. Dong and Y. Qiu, Study on the stability of CH3NH3PbI3 films and the effect of post-modification by aluminum oxide in all-solid-state hybrid solar cells, *J. Mater. Chem. A*, 2014, **2**, 705–710.

57 T. A. Bruton and D. L. Sedlak, Treatment of aqueous film-forming foam by heat-activated persulfate nder conditions representative of in situ chemical oxidation, *Environ. Sci. Technol.*, 2018, **51**(23), 13878–13885.

58 H. V. Lutze, J. Brekenfeld, S. Naumov, C. von Sonntag and T. C. Schmidt, Degradation of perfluorinated compounds by sulfate radicals - New mechanistic aspects and economical considerations, *Water Res.*, 2018, **129**, 509–519.

59 T. A. Bruton and D. L. Sedlak, Treatment of perfluoroalkyl acids by heat-activated persulfate under conditions representative of in situ chemical oxidation, *Chemosphere*, 2018, **206**, 457–464.

60 B. Wu, S. Hao, Y. Choi, C. P. Higgins, R. Deeb and T. J. Strathmann, Rapid destructin and defluorination of perfluorooctanesulfonate by alkaline hydrothermal reaction, *Environ. Sci. Technol. Lett.*, 2019, **6**(10), 630–636.

61 Y. Lee, S. Lo, P. Chiueh, Y. Liou and M. Chen, Microwave-hydrothermal decomposition of perfluorooctanoic acid in water by iron-activated persulfate oxidation, *Water Res.*, 2010, **44**(3), 886–892.

62 X. Dai, Z. Xie, B. Dorian, S. Gray and J. Zhang, Comparative study of PFAS treatment by UV, UV/ozone, and fractionations with air and ozonated air, *Environ. Sci.: Water Res. Technol.*, 2019, **5**(11), 1897–1907.

63 S. Sahu, M. Qanbarzadeh, M. Ateia, H. Torkzadeh, A. Maroli and E. Cates, Rapid degradation and mineralization of perfluorooctanoic acid by a new peititjeanite Bi3O (OH) (PO4) 2 microparticle ultraviolet photocatalyst, *Environ. Sci. Technol. Lett.*, 2018, **5**(8), 533–538.

64 T.-H. Kim, S. Yu, Y. Choi, T.-Y. Jeong and S. D. Kim, Profiling the decomposition products of perfluorooctane sulfonate (PFOS) irradiated using an electron beam, *Sci. Total Environ.*, 2018, **621–632**, 1295–1303.

65 Z. Zhang, J.-J. Chen, X.-J. Lyu, H. Yin and G.-P. Sheng, Complete mineralization of perfluorooctanoic acid (PFOA) by γ-irradiation in aqueous solution, *Sci. Rep.*, 2015, **4**(1), 1–6.

66 K. E. Carter and J. Farrell, Oxidative destruction of perfluorooctane sulfonate using boron-doped diamond film electrodes, *Environ. Sci. Technol.*, 2008, **42**, 6111–6115.

67 G. R. Stratton, F. Dai, C. L. Bellona, T. M. Holsen, E. R. V. Dickenson and S. M. Thagard, Plasma-based water treatment: Efficient transformation of perfluroalkyl substances in prepared solutions and contaminated groundwater, *Environ. Sci. Technol. Lett.*, 2017, **51**(3), 1643–1648.

68 S. Huang and P. Jaffé, Defluorination of perfluorooctanoic acid (PFOA) and perfluorooctane sulfonate (PFOS) by Acidimicrobium sp. Strain A6, *Environ. Sci. Technol.*, 2019, **53**(19), 11410–11419.

69 Y. Gu, W. Dong, C. Luo and T. Liu, Efficient reductive decomposition of perfluorooctanesulfonate in a high photon flux UV/sulfite system, *Environ. Sci. Technol.*, 2016, **50**(19), 10554–10561.

70 M. J. Bentel, Y. Yu, L. Xu, Z. Li, B. M. Wong and Y. Men, *et al.* Defluorination of per- and polyfluoroalkyl substances (PFASs) with hydrated electrons: Structural dependence and implications to PFAS remediation and management, *Environ. Sci. Technol.*, 2019, **53**(7), 3718–3728.

71 Z. Chen, H. Tian, H. Li, J. Li, R. Hong and F. Sheng, *et al.* Application of surfactant modified montmorillonite with different conformation for photo-treatment of perfluorooctanoic acid by hydrated electrons, *Chemosphere*, 2019, 1180–1188.

72 M. Laroussi and F. Leipold, Evaluation of the roles of reactive species, heat, and UV radiation in the inactivation of bacterial cells by air plasmas at atmospheric pressure, *Int. J. Mass Spectrom.*, 2004, **233**(1–3), 81–86.

73 P. Sunka, V. Babický, M. Clupek, P. Lukes, M. Simek and J. Schmidt, *et al.* Generation of chemically active species by electrical discharges in water, *Plasma Sources Sci. Technol.*, 1999, **8**(2), 258.

74 P. Lukes, E. Dolezalova, I. Sisrova and M. Clupek, Aqueous-phase chemistry and bactericidal effects from an air discharge plasma in contact with water: evidence for the formation of peroxynitrite through a pseudo-second-order post-discharge reaction of H2O2 and HNO2, *Plasma Sources Sci. Technol.*, 2014, **23**(1), 015019.

75 P. J. Bruggeman, M. J. Kushner, B. R. Locke, J. G. E. Gardeniers, W. G. Graham and D. B. Graves, *et al.* Plasma-liquid interactions: a review and roadmap, *Plasma Sources Sci. Technol.*, 2016, **25**(5), 053002.

76 K. Tachibana and T. Nakamura, Comparative study of discharge schemes for production rates and ratios of reactive oxygen and nitrogen species in plasma activated water, *J. Phys. D: Appl. Phys.*, 2019, **52**, 385202.

77 B. Jiang, Z. Jingtang, S. Qiu, M. Wu, Q. Zhang and Z. Yan, *et al.* Review on electrical discharge plasma technology for wastewater remediation, *Chem. Eng. J.*, 2014, **236**, 348–368.

78 M. Saleem, O. Biondo, G. Sretenovic, G. Tomei, M. Magarotto and D. Pavarin, *et al.* Comparative performance assessment of plasma reactors for the treatment of PFOA, reactor design, kinetics, mineralization and energy yield, *Chem. Eng. J.*, 2020, **382**, 123031.

79 R. K. Singh, S. Fernando, S. F. Baygi, N. Multari, S. M. Thagard and T. M. Holsen, Breakdown products from perfluorinated alkyl substances (PFAS) degradation in a plasma-based water treatment process, *Environ. Sci. Technol.*, 2019, **53**, 2731–2738.

80 R. Hayashi, H. Obo, N. Takeuchi and K. Yasuoka, Decomposition of perfluorinated compounds in water by DC plasma within oxygen bubbles, *Electr. Eng. Jpn.*, 2015, **190**(3), 767–772.

81 V. Jovicic, M. J. Khan, A. Zbogar-Rasic, N. Fedorova, A. Poser and P. Swoboda, *et al.* Degradation of low concentrated perfluorinated compounds (PFCs) from water samples using non-thermal atmospheric plasma, *Energies*, 2018, **11**, 1290.

82 R. K. Singh, N. Multari, C. Nau-Hix, R. H. Anderson, S. D. Richardson and T. M. Holsen, *et al.* Rapid removal of poly- and perfluorinated compounds from investigation-derived waste (IDW) in a pilot scale plasma reactor, *Environ. Sci. Technol.*, 2019, **53**(19), 11375–11382.

83 I. Chernets, G. Nirenberg, A. Fridman and A. Rabinovich, *Development of high-power plasma reformer and power supply for large scale applications*, 2011.

84 R. D. Robinson, K. Gutsol, A. Rabinovich and A. Fridman, Plasma acid production in a gliding arc plasmatron, *Plasma Med.*, 2012, **2**(4), 249–258.

85 L. Wójcik, B. Szostek, W. Maruszak and M. Trojanowicz, Separation of perfluorocarboxylic acids using capillary electrophoresis with UV detection, *Electrophoresis*, 2005, **26**(6), 1080–1088.

86 M. Tracy, X. Liu and C. Pohl, *Analysis of Perfluorooctane Sulfonate (PFOS) and Perfluorooctanoate (PFOA) in Water Samples Using Reversed-Phase Liquid Chromatography (RPLC) with Suppressed Conductivity Detection*, Thermo Scientific, 2008.

87 N. Daneshvar, A. Aleboyeh and A. R. Khataee, The evaluation of electrical energy per order (EEo) for photooxidative decolorization of four textile dye solutions by the kinetic model, *Chemosphere*, 2005, **59**(6), 761–767.

88 B. N. Nzeribe, M. Crimi, S. M. Thagard and T. M. Holsen, Physico-chemical processes for the treatment of per- and polyfluoroalkyl substances (PFAS): A review, *Crit. Rev. Environ. Sci. Technol.*, 2019, **49**(10), 866–915.

89 P. Rumbach, D. M. Bartels, R. M. Sankaran and D. B. Go, The effect of air on solvated electron chemistry at a plasma/liquid interface, *J. Phys. D: Appl. Phys.*, 2015, **48**(42), 424001.

90 L. Guo, R. Xu, D. Liu, Y. Qi, Y. Guo and W. Wang, *et al.* Eradication of methicillin-resistant Staphylococcus aureus biofilms by surface discharge plasmas with various working gases, *J. Phys. D: Appl. Phys.*, 2019, **52**(42), 425202.

91 G. Fridman, A. D. Brooks, M. Balasubramanian, A. Fridman, A. Gutsol and V. N. Vasilets, *et al.* Comparison of direct and indirect effects of non-thermal atmospheric-pressure plasma on bacteria, *Plasma Processes Polym.*, 2007, **4**(4), 370–375.

92 J. Kolb, A. Mohamed, R. Price, R. Swanson, A. Bowman and R. Chiavarini, *et al.*, Cold atmospheric pressure air plasma jet for medical applications, *Appl. Phys. Lett.*, 2008, **92**, 241501.

93 E. J. Szili, S.-H. Hong, J.-S. Oh, N. Gaur and R. D. Short, Tracking the Penetration of Plasma Reactive Species in Tissue Models, *Trends Biotechnol.*, 2018, **36**(6), 594–602.

94 V. Boiteux, C. Bach, V. Sagres, J. Hemard, A. Colin and C. Rosin, *et al.* Analysis of 29 per- and polyfluorinated compounds in water, sediment, soil and sludge by liquid chromotography-tandem mass spectrometry, *Int. J. Environ. Anal. Chem.*, 2016, **96**(8), 705–728.

95 S. Taniyasu, N. Yamashita, E. Yamazaki, P. Rostkowski, L. W. Yeung and S. K. Kurunthachalam, *et al.* Contamination profiles of perfluorinated chemicals in the inland and coastal waters of Japan following the use of fire-fighting foams, in *Water Challenges and Solutions on a Global Scale*, ACS Symposium Series, 2015, vol. 1206.

96 K. A. Barzen-Hanson, S. C. Roberts, S. Choyke, K. Oetjen, A. McAlees and N. Riddell, *et al.* Discovery of 40 classes of per- and polyfluoroalkyl substances in historical aqueous film-forming foams (AFFFs) and AFFF-impacted groundwater, *Environ. Sci. Technol.*, 2017, **51**(4), 2047–2057.

97 R. K. Singh, L. Philip and S. Ramanujam, Continuous flow pulse corono discharge reactor for the tertiary treatment of drinking water: Insights on disinfection and emerging contaminants removal, *Chem. Eng. J.*, 2019, **355**, 269–278.

98 K. Yasuoka, K. Sasaki, R. Hayashi, A. Kosugi and N. Takeuchi, Degradation of perfluoro compounds and F-

 This journal is © The Royal Society of Chemistry 2020

recovery in water using discharge plasmas generated within gas bubbles, *Int. J. Environ. Sci. Technol.*, 2010, **4**(2), 113–118.

99 S. Li, X. Wang, L. Liu, Y. Guo, Q. Mu and A. Mellouki, Enhanced degradation of perfluorooctanoic acid using dielectric barrier discharge with La/Ce-doped TiO2, *Environ. Sci. Pollut. Res.*, 2017, **24**, 15794–15803.

100 S. B. Shenoy, A. Rabinovich, A. Fridman and H. Pearlman, Process optimization of methane reforming to syngas using Gliding Arc Plasmatron, *Plasma Processes Polym.*, 2019, **16**(4), 1800159.

101 A. Rabinovich, G. Nirenberg, I. Chernets and A. Fridman, High Power Non-Thermal Plasma System for Industrial Applications, *US9216400B2*, 2015.